Aerosol and Air Quality Research, 9: 421-434, 2009

ISSN: 1680-8584 print / 2071-1409 online
doi: 10.4209/aaqr.2009.04.0024

Vertical Profile of Ozone and Accompanying Air Pollutant Concentrations Observed at a Downwind Foothill Site of Industrial and Urban Areas

Kuo-Hsin Tseng[1], Chien-Lung Chen[2], Min-Der Lin[1], Ken-Hui Chang[3], Ben-Jei Tsuang[1*]

[1] *Department of Environmental Engineering, National Chung-Hsing University, Taichung 402, Taiwan*
[2] *Department of Finance, Fortune Institute of Technology, Kaohsiung 831, Taiwan*
[3] *Department of Safety, Health and Environmental Engineering, National Yunlin University of Science and Technology, Taiwan*

ABSTRACT

This study measured vertical distributions of ozone, sulfur dioxide, nitrogen oxide, carbon monoxide, six biogenic-related volatile organic compounds, wind vector, humidity and temperature within the Planetary Boundary Layer (PBL) below 1200 m using a tethered balloon sounding system at a downwind rural site in the Taichung Basin, Taiwan, during the 2002 summer. During ozone episodes, both nocturnal inversion and valley-mountain wind circulation were stronger than those during non-episode days. The observed vertical distributions of these pollutants indicate that the concentrations of carbon monoxide, nitrogen monoxide and biogenic volatile organic compounds decreased as the height increased. Conversely, the highest ozone concentrations were measured during early afternoon at heights of 100-600 m above ground level. Notably, these high ozone concentrations were normally accompanied by relatively higher concentrations of nitrogen dioxide and sulfur dioxide, but not carbon monoxide. From emission inventory, trajectory analysis and statistical analysis, all suggest that high-stack point sources have an important role in causing the summer ozone episodes. This suggestion is supported by 11-y summer data at three stations in the Basin. In addition, it is found that part of the early-afternoon surface ozone was from ozone stored aloft in the residue layer at heights above the nocturnal boundary layer of the preceding night.

Keywords: Tethersonde system; Ozone; Vertical profile; Nocturnal inversion; Valley-mountain wind circulation.

INTRODUCTION

Based on data for the recent decade in central Taiwan, the worst ozone episodes typically occur during autumn and spring (Taiwan EPA, 2003). Nonetheless, summer ozone episodes began monitored since 2002. This study presents the first field campaign data obtained in summer, when a few high ozone episodes occurred. Central Taiwan is of particular interest for air-quality studies, as this region is home to the Taichung Power Plant (TP) and Mailiao Power Plant (MP) (Fig. 1). The TP became operational in 1991, followed by MP in 2001. The TP and MP ranked first and sixth worldwide in terms of the amount of CO_2 they emit, respectively (Tollefson, 2007).

Data for ozone (O_3), sulfur dioxide (SO_2), nitrogen oxide (NO_x), carbon monoxide (CO), methane (CH_4) and non-methane hydrocarbon (NMHC) concentrations were routinely obtained by Taiwan Environmental Protection Administration (EPA) via its air-quality monitoring network in central Taiwan. Although pollutant sources in urban or industrialized areas generate the most pollution, poor air quality is frequently encountered in downwind rural areas (Comrie, 1994; Silibello *et al*., 1998; Debaje and Kakade, 2006; Kumar *et al*., 2008; Yang *et al*., 2008; Yang *et al*., 2008). In particular, ozone and secondary $PM_{2.5}$, typically produced in 30-200 km downwind of precursors NMHCs, NO_x and SO_2 (MacKenzie *et al*., 1995; Lin *et al*., 2008; Kuo *et al*., 2009), are photochemically formed under stagnant meteorological conditions (Oke, 1987; Aneja *et al*., 1994; Vukovich, 1994; Ludwig *et al*., 1995; Seinfeld, 1998; Cheng, 2001; Cheng *et al*., 2001; Devara *et al*., 2005; Hung *et al*., 2005; Wang and Chen, 2008).

Recent studies demonstrated that ozone and its precursors can be stored aloft during the night and mixing downward towards the ground when the ground surface heats up and the nocturnal inversion breaks up in the morning (McElroy and Smith, 1986; Padro *et al*., 1991; Neu *et al*., 1994; Dayan and Koch, 1996; McKendry *et al*., 1997; Pisano *et al*., 1997; Güsten *et al*., 1998; Lehning *et al*., 1998; Seibert *et al*., 2000; Chen *et al.*, 2002; Lin *et al.*, 2007; Lin, 2008). Vertical distributions of ozone and ozone precursors, such as NO, CO and volatile organic compounds (VOCs), were investigated in a few field studies at other locations (Anlauf *et al*., 1994; Bottenheim *et al*., 1997; Güsten *et al*., 1997; Hayden *et al*., 1997; Helmis *et al*., 1997; Pisano *et al*., 1997; Güsten *et al*., 1998; Greenberg *et al*., 1999; Chen *et al*., 2002; Lin *et al*., 2004; Tsai and Tsuang, 2005; Tseng *et al*., 2009). Such data helps in describing dry deposition and removal processes of O_3, explaining the causes of high pollution events (Colbeck and Harrison, 1985), and providing input for initialization, testing and development of atmospheric chemistry models (Hoff *et al*., 1995; Hedley and Singleton, 1997). These data can also be utilized to supply the basic scientific information for clean air strategies (Baumbach and Vogt, 1999).

This study used a tethered balloon to acquire the vertical and temporal distributions of airborne pollutant concentrations and meteorological variables to a height of 1200 m at a rural site in Caotun (120°39′29.1″ E, 23°59′12.1″ N), and 110 m above sea level (ASL) (Fig. 1). The site is located in the foothills of the Taichung Basin, where the pollutant such as ozone was transported (Taiwan EPA, 2003; Chen *et al.*, 2002). This study focused on the major species O_3, CO, SO_2, NO, NO_2 and six VOCs (Isoprene, methacrolein (MACR), methyl vinyl ketone (MVK), limonene, α-pinene and β-pinene) during the summer field campaign in 2002. The relationships of the ozone

* Corresponding author. Tel.: +886-4-22853411;
Fax: +886-4-22862587
E-mail address: tsuang@nchu.edu.tw

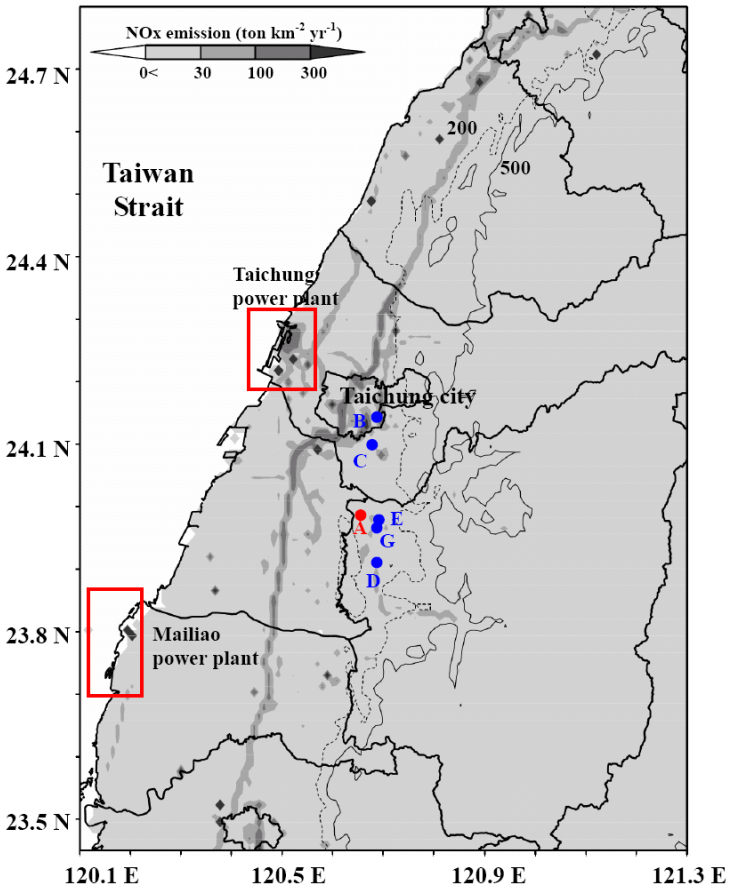

Fig. 1. Map of Central Taiwan shows the study site at Caotun (tethersonde site, A), Taichung (B), Dali (C), Nantou (D), Caotun (E) and Caotun (PAM sit, G). The height contours of 200 m (short dash) and 500 m (solid thin) are also shown. The shaded area represents the NO_x emission, where the dark dots denote pointy sources.

concentration with accompanying pollutants and meteorological conditions are studied. Trajectories and likely reasons for causing the ozone episodes at the foothill site are presented.

DESCRIPTION OF THE STUDY SITE AND FIELD CAMPAIGNS

The field study ran from Aug. 11st-26th, 2002. During this campaign, vertical pollutant concentration profiles and meteorological data were recorded at 3-h intervals—00, 03, 06, 09, 12, 15, 18, 21 Local Time (LT)—except when under the conditions of rain, strong wind (wind speed > 10 m/s) or instrument malfunction, such that during a power failure. The major pollution sources upwind of the study site are local traffic, Taichung City and industrial areas located along the coast. The traffic volume along nearby Express road way 63 was measured on Aug. 29th, 2001. Fig. 2 shows the emission rates for CO, NO_x and SO_2 from the expressway based on traffic volume data. High traffic flow during 7-21 LT on weekdays generated higher CO and NO_x emissions than those during other hours. The CO emission rate was highest, followed by those for NO_x and SO_2. Table 1 lists the emission rates of CO, NO_x and SO_2 from point, line and area sources in the study region (CTCI, 2000). The dry deposition rates and the chemical decay rates for CO, SO_2, NO and NO_2 over land (Hertel *et al*. 1995, Tsuang, 2003; Tsuang *et al*., 2003) are also shown in the table.

Vertical profiles of meteorological variables were recorded at 5-1200 m above ground level (agl) using a tethersonde system (Atmospheric Instrumentation Research, Inc., U.S.A) which

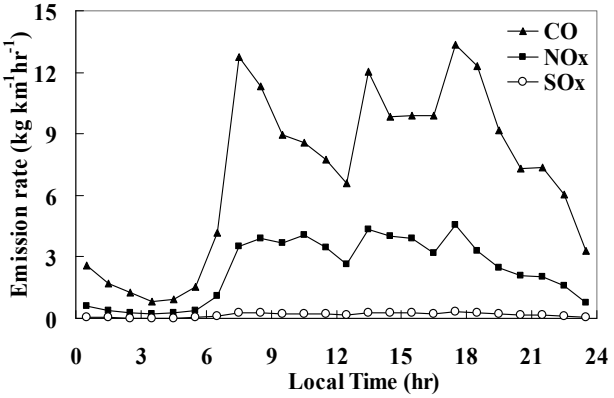

Fig. 2. Vehicle emission rates of CO, NO_x and SO_x at Express road way No.63.

measures temperature, specific humidity, pressure and wind vector. The tethersonde system consists of a balloon with a buoyancy of roughly 9.3 kg, an AIR-TS-3AW winch with tether, an IS-5A-RCR, 403 MHz receiver with a preamp and antenna, laptop computer and a TS-4A-SP-403 tunable sensor package. Balloon height was determined from pressure variations measured by the tethersonde system (Fig. 3).

Vertical distributions of CO, SO_2, NO, NO_2 and O_3 were also determined by the tethersonde system. A specially designed lightweight (600 g) sampling pump with a timer was utilized to

Table 1. Emission, dry deposition rate and chemical decay rate of CO, SO_x and NO_x in the region of 23.5 N to 24.8 N and 120.1 E to 121.3 E.

	CO	SO_x	NO_x
Emission[a] (ton/year) (%)			
Point sources	39,522 (16)	54,963 (92)	89,849 (57)
Line sources	179,965 (73)	1,502 (3)	59,024 (38)
Area sources	27,838 (11)	3,014 (5)	8,335 (05)
Total	247,325 (100)	59,478 (100)	157,208 (100)
Taichung Power Plant	0 (0)	11,706 (20)	31,862 (20)
	CO	SO_2	NO_2
Dry deposition rate (cm/s)[b]	0.01	1	0.1
Chemical decay rate (%/h)[c]	0	7.8	0.75

a: CTCI (2000), b: Hertel *et al.* (1995), c: Tsuang (2003); Tsuang *et al*. (2003)

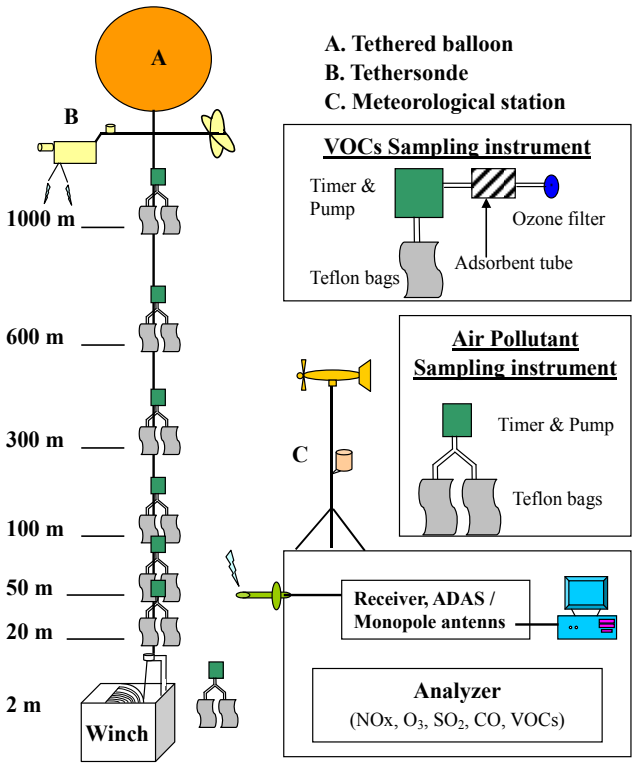

Fig. 3. Schematic diagram for the tethered balloon sampling apparatus used in the field campaign.

inflate two Teflon sampling bags (SKC, Cat #232-08) for sampling heights at 2, 20, 50, 100, 300, 600 and 1000 m agl (Fig. 3). Seven sets of pumps and Teflon sampling bags were mounted along the balloon line for simultaneous profile sampling. After reaching the maximum height, all timers simultaneously started the sampling pumps to inflate Teflon sampling bag pairs. Immediately after sampling, the winch retracted the tether line to retrieve sampling bags. The sampling and descending procedure typically took roughly 50 min. Sampling bags were analyzed using CO, SO_2, NO, NO_2 and O_3 analyzers. O_3 was measured by the TECO analyzer-Model 49 (Thermo Environmental Corporation, Franklin, Massachusetts). NO and NO_2 were measured with a TECO model 42 analyzer. SO_2 and CO was measured using a TECO model 43A and a TECO model 48 analyzer, respectively. The theorem, sample range, detection limit and response time of each analytical instrument shown in Table 2.

Due to the payload limit of a tethersonde system, the vertical and temporal concentration distributions of six VOCs species (isoprene, MACR, MVK, limonene, α-pinene and β-pinene) were sampled using another tethersonde system during daytime (9-18 LT) on Aug. 14th-17th, 2002. These biogenic VOCs were sampled at heights of 2, 10, 100, 200, 400, 600 and 800 m. The sampling instrument had an ozone filter, adsorbent tube, sampling pump and Teflon sampling bag (Fig. 3); Teflon was utilized as the connecting pipeline. An ozone filter was located at the entrance of the gas inlet to eliminate any reactions between ozone and the sample. An adsorbent tube was connected to the ozone filter, and was filled with absorbent Tenax-TA, a porous polymer containing 2, 6-diphenyl-p-phenylene. The Teflon sampling bag and cartridges were installed at the gas outlet for sample collection. The collected samples were analyzed using gas chromatography with a flame ionization detector (FID), a similar procedure to that described by Greenberg *et al*. (1999).

Table 2. Specification of the instrument of each pollutant.

	Ozone	NO/NO_x	SO_2	CO
Type	TECO model 49	TECO model 42	TECO model 43A	TECO model 48
Theorem	U.V. photometric	Chemiluminescence	Pulsed Fluorescence	Gas Filter correlation
Sample range (ppb)	0-1000	0-20000	0-2000	0-1000 ppm
Response time (sec)	20	30	120	30
Detection limit (ppb)	2	0.5	1	0.1 ppm
Precision (ppb)	2	0.5	1	0.1 ppm
Flow (l/min)	1-3	0.65	0.5	1

TECO is Thermo Environment Corporation, Franklin, Massachusetts.

Furthermore, three standard air-quality monitoring stations are located near this study site (Caotun) (Fig. 1), two of which are operated by Taiwan's EPA, that at Dali (120°40′40.0″ E, 24°05′58.1″ N) and Nantou (120°41′8.2″ E, 23°54′46.7″ N) and one at Caotun (120°41′23.12″ E, 23°58′49.53″ N) was operated by the Taiwan Power Company. Additionally, a photochemical assessment monitoring station (PAMS) near Caotun (120°41′18.5″ E, 23°58′44.9″ N) was operated by Taiwan's EPA. At the PAMS, concentrations of 55 VOCs species were measured continuously. Refer to Wang *et al*. (2005) and Yang *et al*. (2005) for additional details of the PAMS. All observed data were utilized to analyze summer ozone episodes during the field campaign.

Calibration of pollutant data consists of two steps. First, all analyzers were calibrated using standard gases (ozone generated by an ozone generator and standard CO, SO_2, NO and NO_x calibration gases) before the field campaign for data quality assurance. Second, the data were further calibrated to offset the adsorption effect in sampling bags. Decay factors for CO, NO, NO_x, SO_2 and O_3 when stored for 5-35 min are 1, 0.94-0.91, 0.93-0.90, 0.91-0.89 and 0.68-0.63, respectively. For further details regarding calibration procedures, see Chen *et al*. (2002).

RESULTS

In total, 107 profile samples were collected and analyzed. Figs. 4-7 shows analytical results. The Pollutant Standard Index (PSI) was used to describe air quality and when the PSI exceeded 100, air quality was unhealthy. The PSI was 100, resulting from a maximum hourly ozone concentration of 120 ppb. Therefore, this study used the ozone concentration for the PSI to define episode periods and non-episode periods. Fig. 4(a) shows the maximum ozone concentration of every vertical profile. The index is 120 ppb. During Aug. 16^{th}-18^{th}, it takes three days in succession and the ozone concentration exceeded 120 ppb, whereas during Aug. 23^{rd} and 25^{th} it did not. Figs. 4(b) and (c) show a similar pattern for ozone concentration at the two EPA stations and study data on surface and at 100 m. Moreover, the time series of other pollutants, such as NO_2 and SO_2, and meteorological conditions had different phenomena in two different periods (Figs. 4(e)-(i) and 4). Therefore, this study denotes the period of Aug. 16^{th}-18^{th} as an ozone episode, and the period of Aug. 23^{rd} and 25^{th} as a non-episode.

Meteorological Conditions

Fig. 5 shows the time series of meteorological variables observed at this study site and nearby stations. Typical diurnal patterns of vertical profiles of potential temperature, wind field and specific humidity were observed at the study site during the episode on Aug. 18^{th} and the non-episode on Aug. 25^{th} (Fig. 6). The wind patterns during episodes and non-episodes differ. The valley-mountain wind circulation that resulted in a northern wind during the day and southern wind during night was stronger on episode days than that on non-episode days. The same wind patterns were also observed at the nearby Caotun station (Fig. 5). During episodes, wind speed at about 600-800 m agl was relatively slow compared to that at heights < 600 m agl. Below 400 m, synoptic wind and mountain wind during episodes came from the south, this southern wind prevailed until 11 LT. The wind then shifted to the north (valley breeze) and lasted until 19 LT. During non-episodes, valley-mountain wind circulation was much weaker and the wind system was controlled by a southwest monsoon. In summer during daylight hours, a northern wind was dominant during episodes, whereas a western wind was dominant during non-episodes (Figs. 5 and 6(a)). At nighttime, a southern wind was dominant during episodes and non-episodes.

The change in the wind direction was accompanied by a change in humidity. During episodes when a valley wind was dominant, specific humidity was roughly 22 g/kg, but decreased to 19 g/kg when a mountain wind was dominant. This is reasonable because downhill wind is generally drier than uphill wind. During non-episodes, specific humidity remained almost constant at approximately 20 g/kg during day and night.

The daily mixing height in ozone episode days were apparently lower than the non-episodic days (Fig. 6). Moreover, the air was more stable during episodes than during non-episodes. During night, the potential temperature gradient at < 100 m was 0.01 K/m during episodes and 0.005 K/m during non-episodes. Thus, the nocturnal inversion was much stronger during episodes than during non-episodes. After sunrise, vertical mixing started at the ground surface and grew to a maximum of roughly 600-800 m in the afternoon during episodes, and to > 1000 m during non-episodes.

CO, SO_2, NO and NO_2 Profiles

Fig. 7 shows the vertical profiles of CO, SO_2, NO (primary pollutants) and NO_2 (secondary pollutant) during episode days and non-episode days, respectively. The concentration ranges of CO, SO_2, NO and NO_2 profiles were approximately 0.6-0.9 ppm, 2-7 ppb, 1-5 ppb and 10-30 ppb, respectively. Table 1 shows that CO had a high emission rate, slow dry deposition velocity and slow chemical-decay rate (Table 1). Moreover, CO is relatively inert; thus, CO has few opportunities to react with other chemical species. Above the nocturnal boundary layer (NBL), the CO concentration exceeded about 0.7 ppm during episodes, slightly higher than the value of 0.6 ppm during non-episodes. During episodes, which were usually under calm wind and stable conditions, the lifetimes of pollutants are much longer than during non-episodes (Tsuang and Chao, 1997; 1999).

In contrast, the chemical decay rates for SO_2 and NO are significantly higher than that of CO. Both SO_2 and NO rapidly reached a pseudo steady state, and converted to sulfate and NO_2, respectively. The NO_2 profiles are consistent with the fact that NO_x ($NO + NO_2$) has the second largest emission rate (Fig. 2), and NO_2 has the second slowest chemical decay rate. Interestingly, during episodes, peak concentrations of SO_2 and

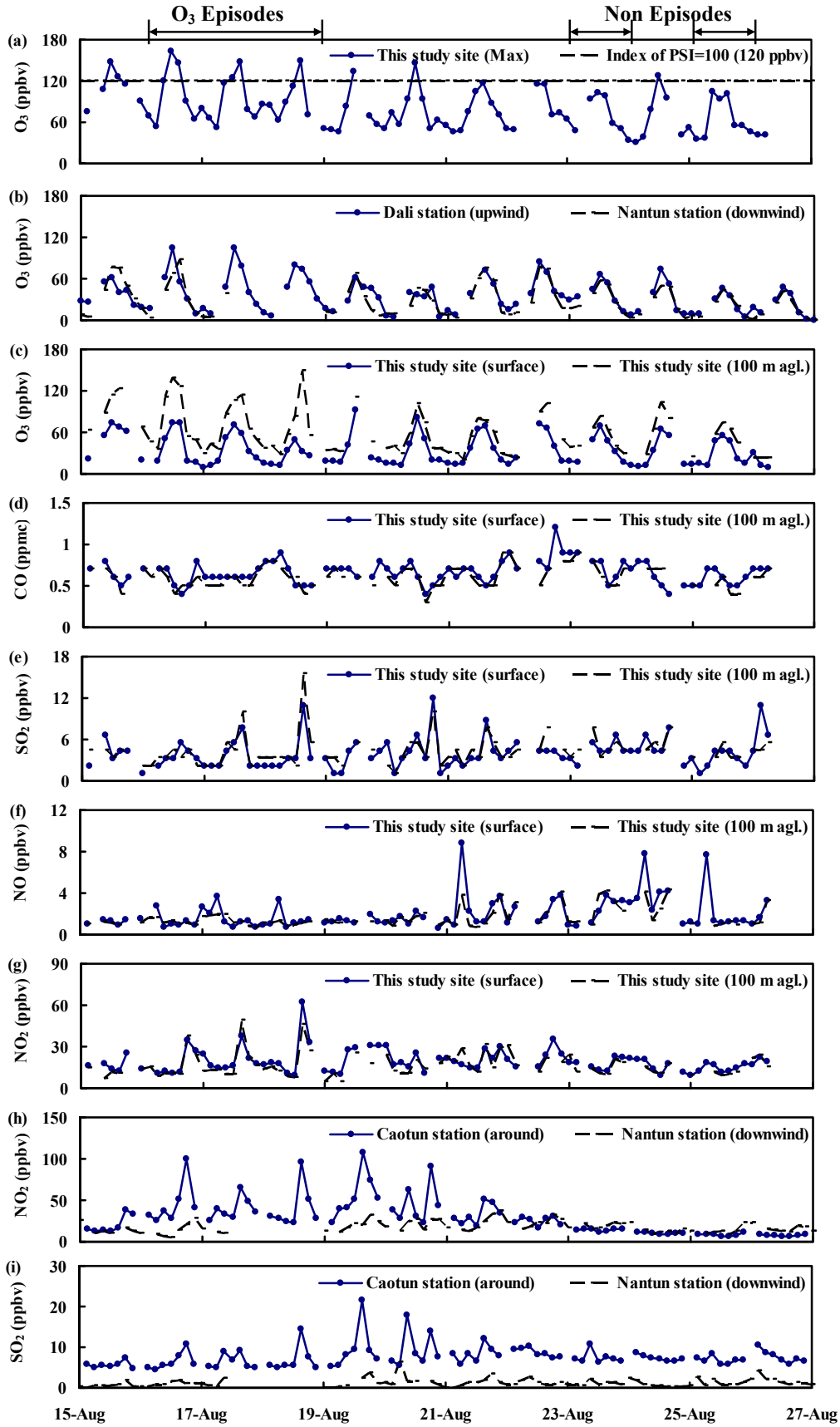

Fig. 4. The time series of pollutants concentration (a) the maximum ozone concentration of every vertical profile and the index is 120 ppb. (b) ozone for EPA station (Dali and Nanton). (c) ozone, (d) CO, (e) SO_2, (f) NO and (g) NO_2 for this field study on surface (2 m agl) and at 100 m agl; (h) NO_2 and (i) SO_2 for air quality monitoring stations (Caotun and Nanton).

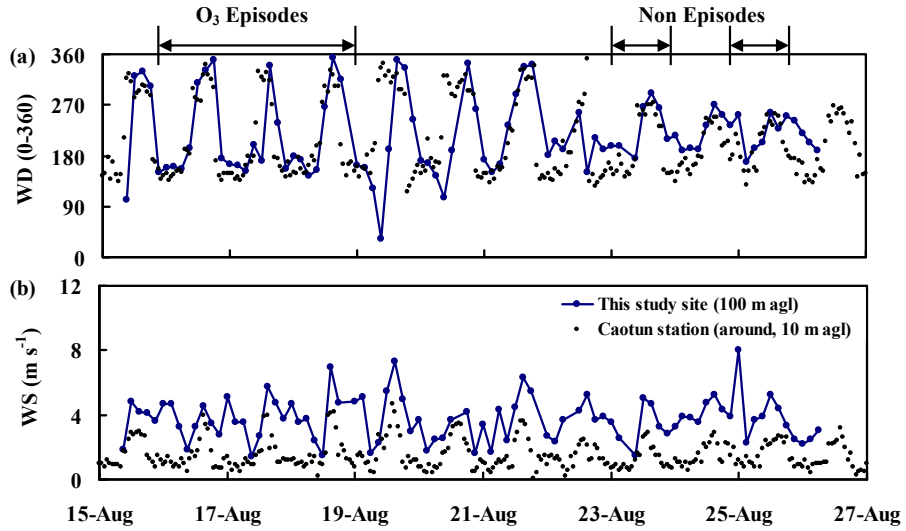

Fig. 5. The time series of meteorological conditions, where (a) WD and (b) WS at this study site (100 m agl) and Caotun station respectively.

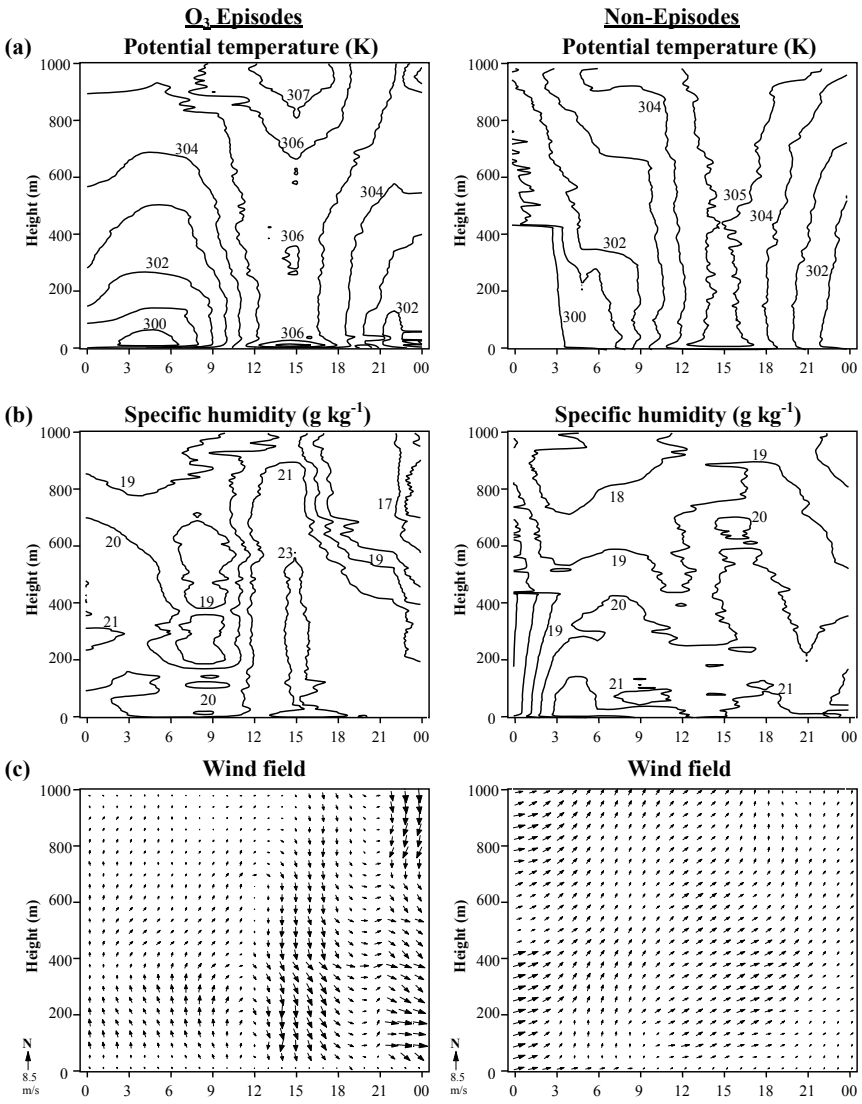

Fig. 6. Profiles of meteorological conditionson an episode (18th Aug., 2002) and a non-episode (25th Aug., 2002) at the study site, where the x-axis represents the local time (hour). (a) potential temperature, (b) specific humidity and (c)wind field.

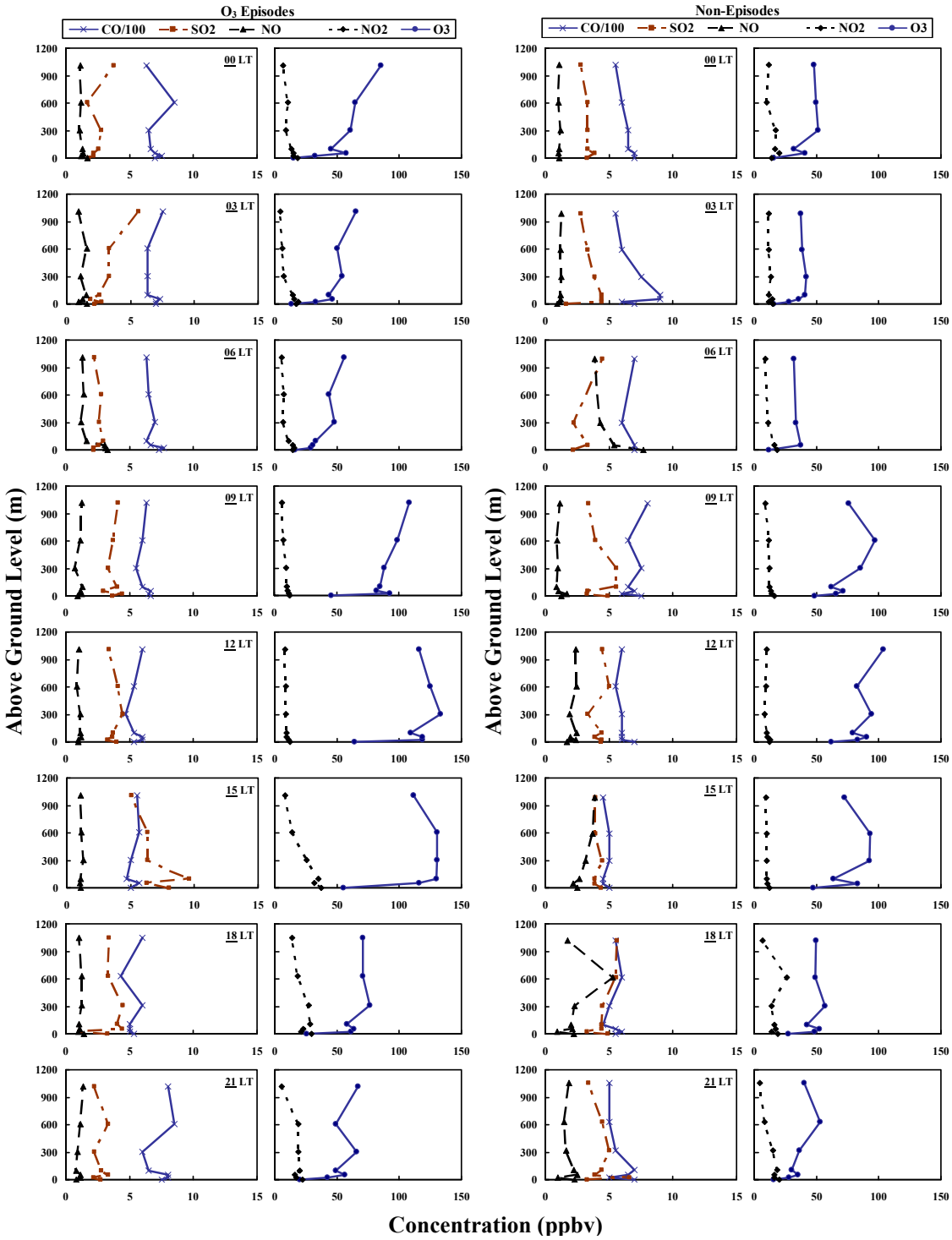

Fig. 7. Composites of the profiles of CO, SO_2, NO, NO_2 and O_3 on episodes (16^{th}-18^{th} Aug., 2002) and non-episodes (23^{rd} and 25^{th} Aug., 2002).

NO_2 were typically found at 100 m agl at 15 LT; however, no such peaks were found for CO.

The vertical structure of profiles of the four pollutants vary greatly in the lower part of the PBL (< 70 m height) and remain almost constant above 200 m agl. The lowest part (< 10-20 m) is called the canopy layer (or deposition layer); the second lowest part (20-70 m height) is the inertial sub layer; and the upper part (70-1000 m) is the mixed layer (Stull, 1988). Within the inertial sub layer, vertical profile gradients for inert pollutants are controlled mainly by their vertical fluxes (Businger *et al*., 1971), which are functions of dry deposition and emission rates. In the mixed layer, all inert pollutants are considered well mixed. The profiles shown are in consistent with an understanding of the vertical structure of PBL.

Ozone Profile

Fig. 7 presents ozone vertical profiles during episode days and non-episode days, respectively. These profiles demonstrate that

O_3 concentrations decreased rapidly toward the ground. This is because surface O_3 was partly removed by deposition and reactions with NO at the surface. During episodes, concentrations at elevated levels were higher than those near the surface, reaching nearly 140 ppb at 100-300 m agl at noon and in the early afternoon. The time series of O_3 vertical profiles, the concentrations at all heights of vertical profiles increased from 9 to 15 LT and, then, returned to their original values in the afternoon, which swing like a pendulum (Chen *et al*., 2002). These concentration profiles indicate that photochemical production and convection were stronger at noon and early afternoon than later in the nightfall and evening. When stable nocturnal inversions formed and NO emissions increased in evening rush hours (roughly 18 LT) (Fig. 2), air masses were constrained in the NBL and ozone was rapidly depleted due to dry deposition and chemical reaction with NO. During night, surface O_3 dramatically decreased due to a continuous depletion process, and a relatively higher O_3 concentration was sustained above the NBL.

During non-episodes, pattern of O_3 vertical profiles and the time series resembled those during episodes. The concentration of O_3 at high altitudes was also higher than that at the surface and peak O_3 concentrations reached only around 90 ppb at 12-15 LT. Unlike the vertical profiles experienced during episodes, the ozone concentration decreased smoothly near the surface during non-episodes. During night, the elevated O_3 concentration had little effect on the emitted NO, which was confined within the NBL and, thus, preserved its high concentration.

Biogenic Related VOCs Profiles

Fig. 8 presents the biogenic VOCs vertical profiles. The VOCs concentrations were high at noon and in the early afternoon and relatively lower during morning and evening hours. Samples obtained near the surface had the greatest VOCs concentrations, which eventually decreased as the height increased. In particular, maximum concentrations of isoprene and its oxidized products (MACR and MVK) occurred at the surface and markedly decreased at heights up to 100 m. In contrast, the VOCs concentrations varied slightly above 100 m. The concentration gradients of isoprene and its oxidized products (MACR and MVK) profiles were approximately 0.2-1.8 ppb, 1-5 ppb and 2-18 ppb, respectively. The vertical profiles of limonene, α-pinene and β-pinene had a similar trend. Since the vertical profiles of the biogenic VOCs did not show peaks within 100-300 m agl, as observed in ozone profile in the early afternoon (Fig. 7), it is unlike for biogenic VOCs to be main precursor causing the ozone peaks within the 100-300 m agl height range.

DISCUSSION

Residual Ozone Layer and Downward Mixing Effect

When the atmospheric turbulence was strong in the afternoon, surface O_3 concentration reached the maximum and O_3 concentration at high altitude is also up to the maximum. The ozone at high altitude can remain above the mixing layer and NBL through to the next early morning and these O_3 will contribute to O_3 concentrations in the daytime next day. This layer is so-called residual ozone layer (Neu *et al.*, 1994) and the phenomena have also been observed in Southern Taiwan (Lin *et al.*, 2007; Lin, 2008). In this study, daily maximum mixed layer was about 750 m agl in the episode day and more than 1000 m agl in the non-episode day (Fig. 6). The result of the maximum mixed layer was about 750-1700 m agl during this field campaign. During episode days, the ozone concentration at 1000 m agl remained relatively high at night (Fig. 7). This phenomenon indicates that ozone and its precursors can be stored aloft during the night. Fig. 9 shows the correlations between O_3 concentrations at 100 m agl at 15 LT and O_3 concentrations

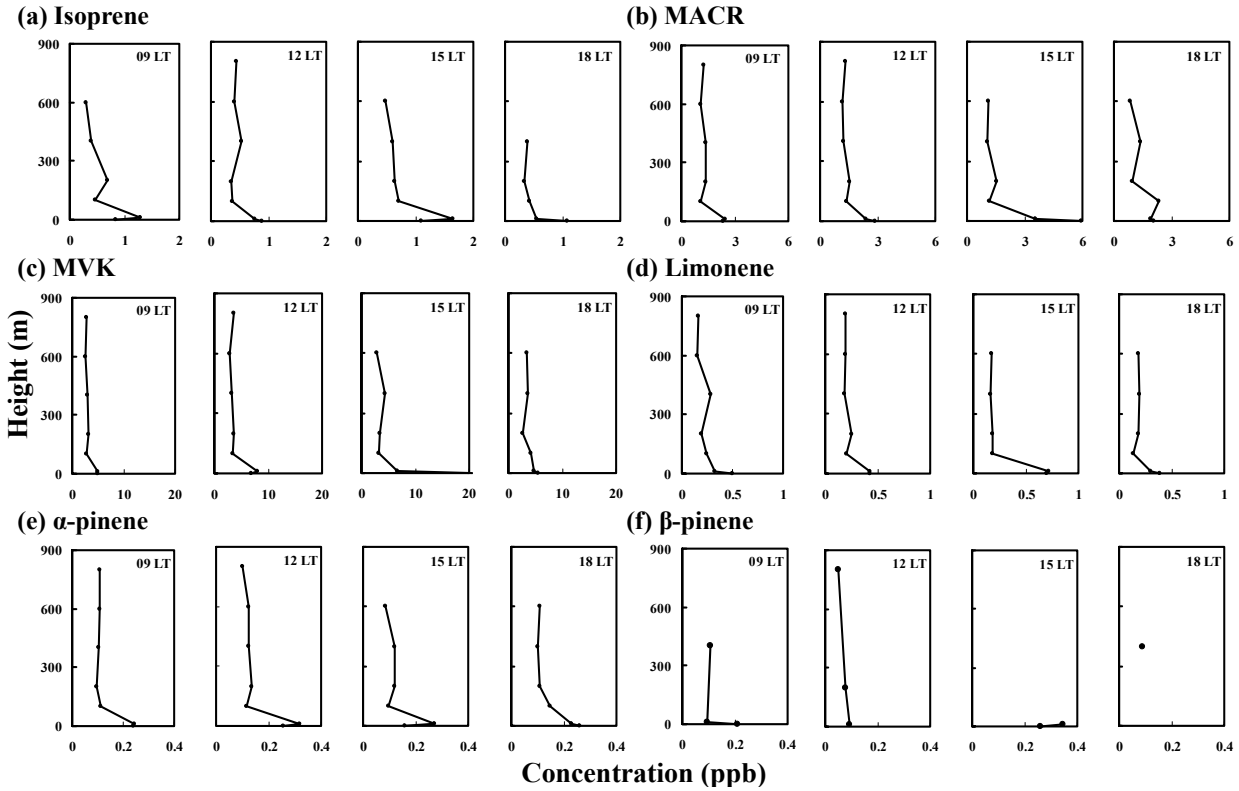

Fig. 8. Profiles of biogenic VOCs in the daytime (9LT~18LT) during 14th-17th Aug., 2002. (a) Isoprene, (b) Methacrolein (MACR), (c) Methyl vinyl ketone (MVK), (d) Limonene, (e) α-pinene and (f) β-pinene.

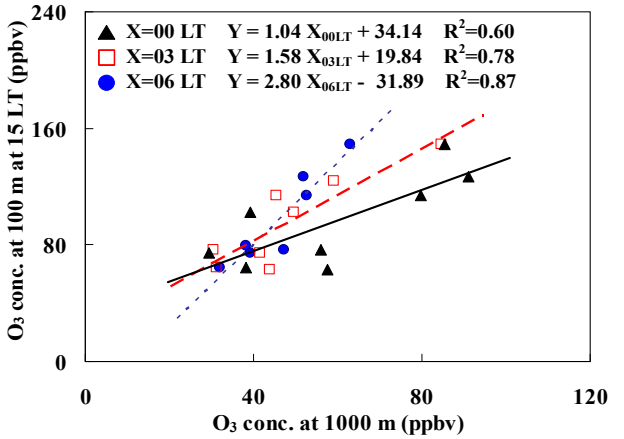

Fig. 9. X-Y plots of the O_3 concentrations at 15 LT at 100 m agl with the O_3 concentrations in the previous 9, 12, 15 hours at 1000 m agl.

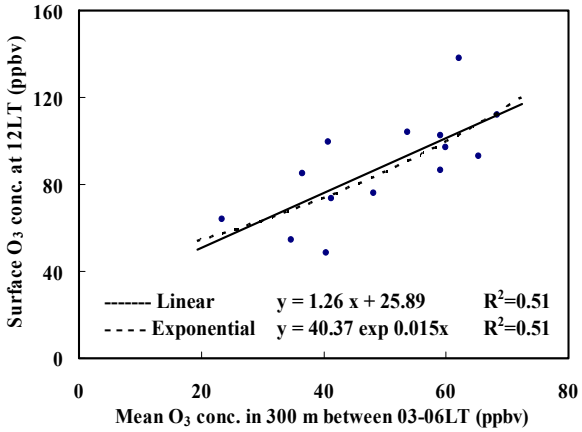

Fig. 10. Relationship between the average O_3 concentration at 300 m agl between 03-06 LT and the ozone concentration on the ground (the average of 2 m and 20 m agl) at 12 LT at the study site (Caotun).

during the previous 9, 12, 15 h (06 LT, 03 LT, 00 LT) at 1000 m agl, with r^2 values of 0.87, 0.78 and 0.60, respectively. This result indicates that ozone concentrations at heights above the nocturnal boundary layer were correlated with the ozone concentration at 100 m agl in the following afternoon.

During the early morning hours, the ozone concentrations increase as the altitudes increase to maximum mixing depth. Therefore, the residual ozone can be downward-mixed to the ground and increase surface ozone concentration. Aneja *et al.* (2000) developed an empirical relationship between maximum O_3 concentration measured at the surface during the day and the previous night's average ozone concentration in the residual layer. Similarly, this study utilized measured 13 data sets to analyze the downward mixing effects. Fig. 10 shows the correlation between observed maximum surface ozone concentration (C_{0Max}) at 12 LT. and early morning average ozone concentration above the NBL($\overline{C}_{aNBL}$) at 03-06 LT. The linear and exponential regression lines fit data well with the determination of correlation (r^2) of 0.51 and 0.51, respectively (Table 3). The magnitude of the exponent/slope is the contribution of ozone above the NBL mixing downward toward ground level. The intercept can be understood as the background O_3 concentration, which, along with its precursors in the residual layer, did not impact the surface ozone concentration. Empirical linear regression estimates indicate that the background ozone concentration at Caotun (central Taiwan) was 26 ppb during the test period.

High Ozone Concentrations Accompanied Pollutants

The vertical profile data shows that the ozone concentration peaked at 100-600 m agl (Fig. 7). Experimental data demonstrate that ozone concentration is correlated with precursors (NO, NO_2, VOCs) and ozone concentrations at 1000 m agl at night. Therefore, the relationship between ozone concentration at noon at 100 m agl ($O_3^{100,12}$) and its precursors can be written as

$$O_3^{100,12} = f(NO^{S,12}, NO_2^{S,12}, VOC_{g2}^{S,12}, NO^{100,12}, NO_2^{100,12}, SO_2^{100,12}, CO^{100,12}, O_3^{1000,0}, O_3^{1000,3}, O_3^{1000,6}) \quad (1)$$

where CO, NO, NO_2, SO_2, VOCs and O_3 is concentration for each variable in ppb. Superscripts "s" and "100" denote that a variable was measured at the surface and 100 m agl, respectively. The second superscript (0, 3, 6, 12) denotes LT (00, 03, 06, 12 LT) for the ozone concentration at 1000 m agl in the early morning. $VOC_{g2}^{S,12}$ is the sum of the styrene and cyclohexane concentrations at the surface, which are better correlated (r^2 is 0.34 and 0.49, respectively) than other VOCs species with the ozone concentration at 100 m agl (Fig. 11). Ten-day data records were used for analysis. Stepwise multiple-linear regression analysis indicates that only variables $O_3^{1000,0}$, $SO_2^{100,12}$, $VOC_{g2}^{S,12}$ and $NO^{S,12}$ have statistically significant effects in the equation. Thus, the relationship is determined as

$$O_3^{100,12} = 1.90(\pm 0.18)\cdot O_3^{1000,0} + 28.21(\pm 2.83)\cdot SO_2^{100,12} + 22.22(\pm 3.28)\cdot VOC_{g2}^{S,12} + 16.34(\pm 2.81)\cdot NO^{S,12} - 207.66(\pm 29.08) \quad (2a)$$

$$O_3^{*100,12} = 1.54\cdot O_3^{*1000,0} + 1.24\cdot SO_2^{*100,12} + 0.72\cdot VOC_{g2}^{*S,12} + 0.63\cdot NO^{*S,12} \quad (2b)$$

Table 3. Empirical regression equations for the ozone downward mixing effect.

reference/ Periods of study	Study site	Linear Eq. $C_{0Max} = a + b\,\overline{C}_{aNBL}$			Exponential Eq. $C_{0Max} = a\exp(b\,\overline{C}_{aNBL})$		
		a (ppb)	*b*	r^2	*a* (ppb)	*b* (1/ppb)	r^2
Aneja *et al.* (2000) summer 1993-1997	Auburn, NC, USA	28.13	0.75	0.42	27.67	0.016	0.41
Chen *et al.* (2002) winter 1999-2001	Caoton, Nantou, Taiwan	29.07	0.91	0.49	32.92	0.017	0.49
This study summer 2002	Caoton, Nantou, Taiwan	25.87	1.26	0.51	40.37	0.015	0.51

$\overline{C}_{0Max}$: maximum surface ozone at daytime
$\overline{C}_{aNBL}$: the early morning average ozone concentration above NBL

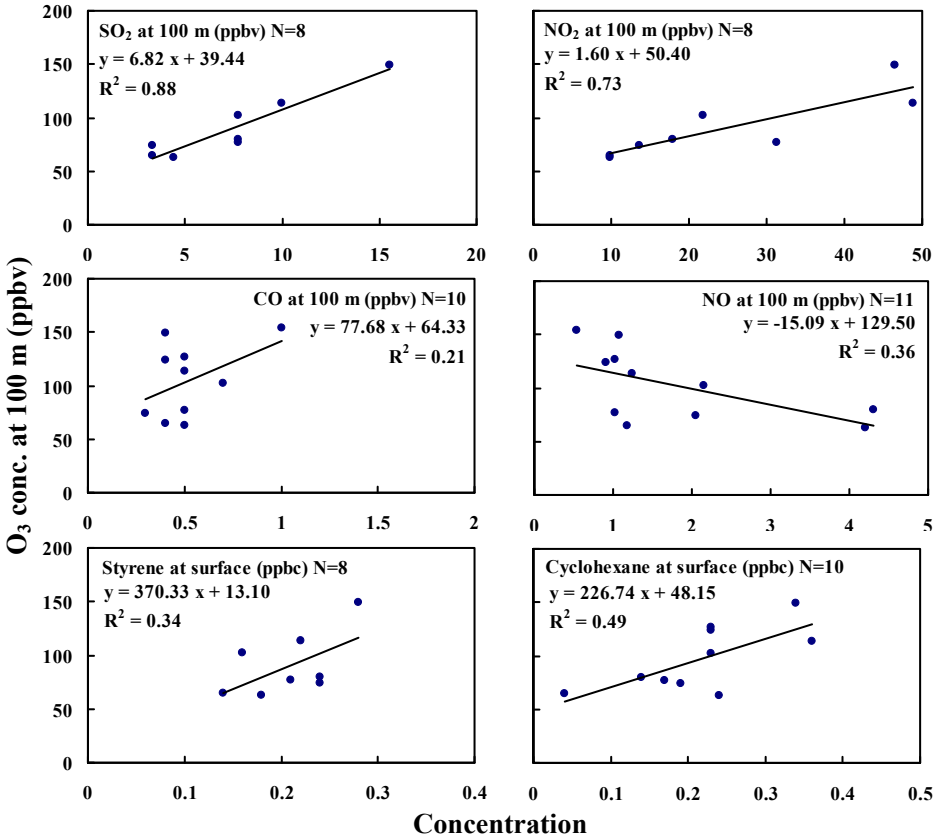

Fig. 11. Correlation of 100-m ozone concentration with the concentrations of 100-m SO_2, 100-m NO_2, 100-m CO, 100-m NO, surface Styrene and surface Cyclohexane at 15 LT during the field campaign.

Eq. (2a) is in the normal units (ppb), and Eq. (2b) is in standardized form, where superscript * denotes the variable in the standardized form. For example, $O_3^* \equiv (O_3 - \overline{O_3})/\sigma(O_3)$, where the overbar "—" denotes the mean of the variable, and σ is the standard deviation. The p-value of all variables are < 0.002, meaning that these coefficients are statistically significant. Fig. 12 presents a comparison between observed and predicted $O_3^{100,12}$ during the campaign period, which has an r^2 of 0.85 (Eq. 2).

The above statistical analysis (Eq. 2) indicates that $SO_2^{100,12}$ is correlated with $O_3^{100,12}$. Nonetheless, SO_2 is not a precursor for ozone production. Notably, SO_2 is mainly released into the troposphere from high-stack sources, for example, roughly 92% of SO_x and 57% of NO_x was emitted from point sources in the study region (Table 1). And the emission is always accompanied with NO_x. Hence, the high ozone concentration is likely related to high-stack sources. Lin *et al.* (2007) also observed that during an ozone episode, a very high ozone peak was stored aloft in Southern Taiwan; they suspected the high peak likely resulted from an elevated large point source. Moreover, ozone formation has also been observed in power plant plumes in USA by aircrafts (Ryerson *et al.*, 2001). The vertical profiles show that the maximum ozone concentrations occurred around 15 LT at an altitude of 100 m, the NO_2 and SO_2 profiles also peaked at the same time during episode days (Aug. 16-18) (Figs. 4 and 7). Strong correlations exist between the ozone concentration and the NO_2 and SO_2 concentrations at 100 m agl with an r^2 of 0.73 and 0.88, respectively (Fig. 11). However, $NO_2^{100,12}$ is not chosen as a variable in Eq. (2), which is due to the collinearity (Neter *et al.*, 2004) between $SO_2^{100,12}$ and $NO_2^{100,12}$ in regression analysis. Note that $NO_2^{100,12}$ was highly correlated with $SO_2^{100,12}$ with r^2 of 0.76, but $SO_2^{100,12}$ has been chosen in Eq. (2). Conversely, the correlation between the ozone concentration and CO concentration has a low r^2 value of 0.21. In the study region, 73% of CO was emitted from mobile sources (Table 1). Therefore, we conclude that the high ozone concentrations at 100 m agl at the study site were associated more with stack sources than line sources. Note that stack sources (such as nearby power plants) emit both high volumes of SO_2 and NO_x pollutants, whereas line sources only emit high volumes of NO_x and relatively less SO_2.

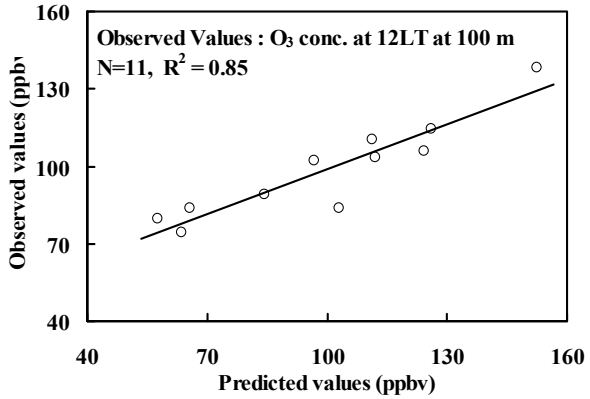

Fig. 12. Comparisons between observed and predicted values for 100-m ozone concentration at 12 LT by Eq. (2) during the field campaign.

Backward Trajectory Analysis

Only line sources and no important point sources exist within a 30-km radius of the study site (Fig. 1). Fig. 13 shows the trajectories, calculated by the GT_x model developed by Tsuang

(2003), to the site during 09-12 LT on episode/non-episode days. On episode days (Fig. 13(a)) wind speeds were markedly slower than those during non-episode days, and local circulations, such as land (E)/sea (W) breeze and valley (N)/mountain (S) wind, accompanying the SE monsoon wind caused the trajectories to spiral toward the study site. The trajectories sweep the source pollution along the coast—from power plants (such as TP) and to inland foothill areas, such as the study site. Many point sources were located along the trajectory routes (Fig. 1). In contrast, during non-episode days (Fig. 13(b)), local circulations were not significant and wind speeds were very fast, hence, few sources were carried in the air parcel. Much less point sources were located along trajectory routes during the non-episodes than the episodes. The episodes of particulate matter were also found occurred under strong land-sea breeze conditions in the Basin (Tsuang *et al.*, 2003).

Verification

In the above sections, it is suspected that high-stack point sources have an important role in causing the summer ozone episodes in the Basin. Nonetheless, the inference is not well supported because the data is not enough. Note that we only have 12-day O_3 and SO_2 profile data during the campaign. In order to test the hypothesis, we use 11-y summer (June, July and August) daily data at 3 TW/EPA stations (Dali, Nantou and Jhushan) from 1996 to 2006 for further analysis. The total data number is 2523 station days. According to the Principal component analysis (PCA) with varimax normalization (Table 4), it can be seen that

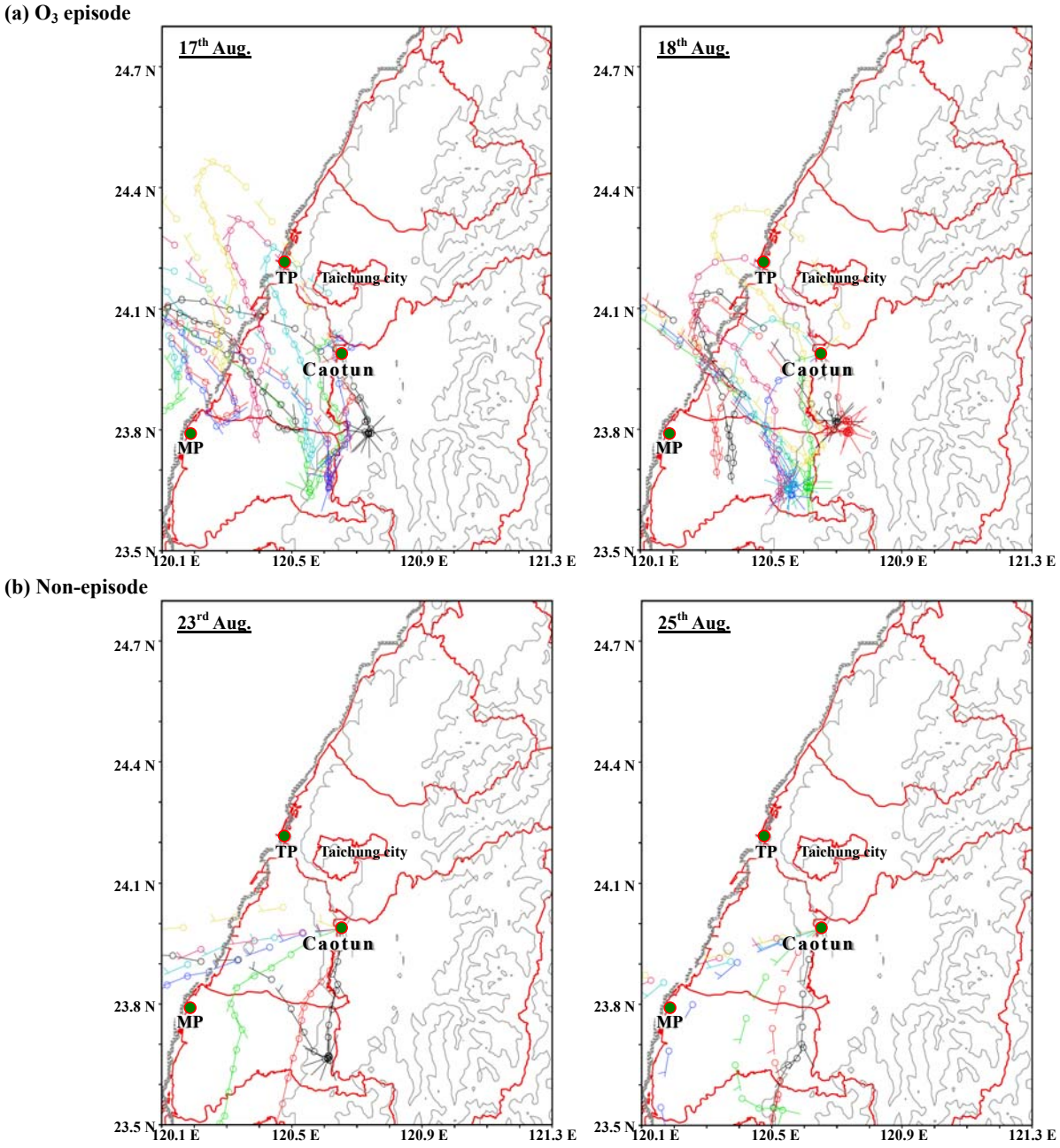

Fig. 13. Backward trajectories from the study site in Caotun on episodes (17th and 18th Aug., 2002) and non-episode (23rd and 25th Aug., 2002), where TP denotes Taichung power plant, and MP denotes Mailiao power plant. The black line denotes trajectories at 09 LT, red at 10 LT, green at 11 LT, blue at 12 LT, light blue at 13 LT, magenta at 14 LT and yellow at 15 LT.

Table 4. Principal component analysis among surface air quality data at Dali, Nantou and Jhushan station during the summer from 1996 to 2006.

Factor	Positive	Negative	%
Factor 1	$\underline{O_3^{E30,\max}}$, $\underline{O_3^{E30,avg}}$, $\underline{SO_2^{E30,avg}}$ $\underline{O_3^{E36,\max}}$, $\underline{O_3^{E36,avg}}$, $\underline{SO_2^{E36,avg}}$ $\underline{O_3^{E69,\max}}$, $\underline{O_3^{E69,avg}}$, $\underline{SO_2^{E69,avg}}$	$\underline{NO^{E30,avg}}$ $\underline{NO^{E36,avg}}$ $\underline{NO^{E69,avg}}$	57.1
Factor 2	$\underline{CO^{E30,avg}}$, $\underline{NO_2^{E30,avg}}$, $\underline{NO_X^{E30,avg}}$ $\underline{CO^{E36,avg}}$, $\underline{NO_2^{E36,avg}}$, $\underline{NO_X^{E36,avg}}$ $\underline{CO^{E69,avg}}$, $\underline{NO_2^{E69,avg}}$, $\underline{NO_X^{E69,avg}}$		42.9
			100.0

Note:
A^B : The superscripts "E30", "E36" and "E69" denote a variable to be measured at Dali (EPA030), Nantou (EPA036) and Jhushan (EPA069) air quality monitoring stations respectively.
Max, Avg: the maximum value and average value
__ shows species correlates to its respective PCA factor with $r^2 > 0.4$
E30, E36, E69: air quality monitoring stations in Dali (EPA030), Nantou (EPA036) and Jhushan (*EPA069).

the daily maximum O_3 concentration and the daily mean O_3 concentration are in the same group (Factor 1) as the daily SO_2 concentration for all the three stations, and their signs of the factor loadings are the same. In contrast, the daily CO concentration is in the same group (Factor 2) as the daily NO_2 concentration. It further confirms that high O_3 concentration is more associated with point sources since 92% again of SO_x was emitted from point sources in the study region. Moreover, the daily NO concentration is, although, in the same group as the O_3 concentration, but their signs of the factor loadings are opposite. It implies that the immediate-upwind emission of NO reduces O_3 concentrations at the three stations in general, likely due to the titration effect (e.g., Chou *et al.*, 2006). Note that the life time of NO concentration is very short, only about an hour (Seinfeld and Pandis, 1998). And there are not many point sources near the three stations. Most of the NO emission near the stations was from mobile sources (Figs. 1 and 2).

CONCLUSIONS

This study investigated the vertical distribution of air pollutants and the state of meteorological variables using two tethered balloon system during the 2002 summer in central Taiwan. The observed profile pattern shows a marked vertical convective mixing under unstable atmospheric boundary layers during daylight hours. The nocturnal inversion and valley-mountain wind circulation during episodes were stronger than those during non-episode days.

The concentration profiles of O_3 demonstrate that O_3 concentrations decreased rapidly toward the ground. The photochemical production and convection were stronger at noon and early afternoon than later in the nightfall. During the episode days, the elevated O_3 concentration was confined within the NBL and, thus, preserved its high concentration at nighttime. The emission inventory, trajectory analysis, statistical analysis and empirical relationships indicate that the ozone formed at the foothill study site on episode days were associated more with stack sources than line sources. This suggestion is supported by 11-y summer data at three stations in the Basin.

ACKNOWLEDGMENTS

The authors are grateful for financial support from the National Science Council, Taiwan, under the contracts NSC-91-EPA-Z-005-004, NSC-92-2211-E-005-023, NSC-93-2211-E-005-006, NSC-94-2211-E-005-039, NSC 95-EPA-Z-005-001 and NSC 95-2111-M-005-001. Thanks to Dr. Arumugam Alagesan, Dr. Andrew Keats and Dr. Ted Knoy for proof reading. We are also grateful to Pei-Hsuan Kuo, Ding-Cang Kuo, Mei-Chun Kuo. Jun-Nan Kuo, Co-Zi Yen and Yu-Chi Kuo for their assistance with the tethersonde operation.

REFERENCES

Aneja, V.P., Li, Z. and Das, M. (1994). Ozone Case Studies at High Elevation in the Eastern United States. *Chemosphere.* 29: 1711-1733.

Aneja, V.P., Mathur, R., Arya, S.P., Li, Y., Murray, G.C., Jr. and Manuszak, T.L. (2000). Coupling the Vertical Distribution of Ozone in the Atmospheric Boundary Layer. *Environ. Sci. Technol*. 34: 2324-2329.

Anlauf, K.G., Mickle, R.E. and Trivett, N.B.A. (1994). Measurement of Ozone during Polar Sunrise Experiment 1992. *J. Geophys. Res.* 99: 25345-25353.

Baumbach, G. and Vogt, U. (1999). Experimental Determination of the Effect of Mountain-Valley Breeze Circulation on Air Pollution in the Vicinity of Freiburg. *Atmos. Environ.* 33: 4019-4027.

Bottenheim, J.W., Brickell, P.C., Dann, T.F., Wang, D.K., Hopper, F., Gallant, A.J., Anlauf, K.G. and Wiebe, H.A. (1997). Non-Methane Hydrocarbons and CO during PACIFIC '93. *Atmos. Environ*. 33: 2079-2087.

Businger, J.A., Wyngaard, J.C., Izumi, Y. and Bradley, E.F. (1971). Flux-Profile Relationships in the Atmospheric Surface Layer. *J. Atmos. Sci.* 28: 181-189.

Carter, W.P.L. (1994). Development of Ozone Reactivity Scales for Volatile Organic Compounds. *J. Air Waste Manage. Assoc.* 44: 881-899.

Chen, C.L., Tsuang, B.J., Tu, C.Y., Cheng, W.L. and Lin, M.D. (2002). Wintertime Vertical Profiles of Air Pollutants over a Suburban Area in Central Taiwan. *Atmos. Environ.* 36: 2049-2059.

Cheng, W.L. (2001). Synoptic weather patterns and their Relationship to High Ozone Concentrations in the Taichung Basin. *Atmos. Environ.* 35: 4971-4994.

Cheng, W.L., Pai, J.L., Tsuang, B.J. and Chen, C.L. (2001).

Synoptic Patterns in Relation to Ozone Concentrations in West-Central Taiwan. *Meteorol. Atmos. Phys.* 78: 11-21.

Chou, Charles C.K., Liu, S.C., Lin, C.Y., Shiu, C.J. and Chang, K.H. (2006). The Trend of Surface Ozone in Taipei, Taiwan, and Its Origins: Implications for Ozone Control Strategies. *Atmos. Environ.* 40: 3898-3908.

Colbeck, I. and Harrison, R.M. (1985). Dry Deposition of Ozone: Some Measurements of Deposition Velocity and of Vertical Profiles to 100 Metres. *Atmos. Environ.* 19: 1807-1818.

Comrie, A.C. (1994). A Synoptic Climatology of Rural Ozone Pollution at Three Forest Sites in Pennsylvania. *Atmos. Environ.* 28: 1601-1614.

CTCI Corporation (2000). Prework for Pursuing Total Load Control of Air Pollution and Standard Method Establishment for Estimating Air Pollutant Emissions. R.O.C. Environmental Protection Agency, Taipei, Taiwan, R.O.C. (in Chinese).

Dayan, U. and Koch, J. (1996). Ozone Concentration Profiles in the Los Angeles Basin- A possible Similarity in the Build-Up Mechanism of Inland Surface Ozone in Israel. *J. Appl. Meteor.* 35: 1085-1090.

Debaje, S.B. and Kakade, A.D. (2006). Weekend Ozone Effect over Rural and Urban Site in India. *Aerosol Air Qual. Res.* 6: 322-333.

Devara, P.C.S., Saha, S.K., Ernest R.P., Sonbawne, S. M., Dani, K.K., Tiwari, Y.K. and Maheskumar, R.S. (2005). A Four-Year Climatology of Total Column Tropical Urban Aerosol, Ozone and Water Vapor Distributions over Pune, India. *Aerosol Air Qual. Res.* 5: 103-114.

Environmental Protection Administration, Taiwan (EPA/Taiwan) (2003). Air Quality Annual Report Taiwan Area in 2002. EPA Publication GPN 2008400070, Taiwan Environmental Protection Administration, Taipei, p. 218.

Greenberg, J.P., Guenther, A., Zimmerman, P., Baugh, W., Geron, C., Davis, K., Helmig, D. and Klinger, L.F. (1999). Tethered Balloon Measurements of Biogenic VOCs in the Atmospheric Boundary Layer. *Atmos. Environ.* 33: 855-867.

Güsten, H., Heinrich, G. and Sprung, D. (1998). Nocturnal Depletion of Ozone in the Upper Rhine Valley. *Atmos. Environ.* 32: 1195-1202.

Güsten, H., Heinrich, G., Mönnich, E., Weppner, J., Cvitaš, T., Klasinc, L., Varotsos, C.A. and Asimakopoulos, D.N. (1997). Thessaloniki '91 Field Measurement Campaign–II. Ozone Formation in the Greater Thessaloniki Area. *Atmos. Environ.*, 31: 1115-1226.

Hayden, K.L., Anlauf, K.G., Hoff, R.M., Strapp, J.W., Bottenheim, J.W., Wiebe, H.A., Froude, F.A., Martin, J.B., Steyn, D.G. and McKendry, I.G. (1997). The Vertical Chemical and Meteorological Structure of the Boundary Layer in the Lower Fraser Valley during PACIFIC '93. *Atmos. Environ.* 31: 2089-2105.

Hedley, M. and Singleton, D.L. (1997). Evaluation of an Air Quality Simulation of the Lower Fraser Valley-I. Meteorology. *Atmos. Environ.* 31: 1605-1615.

Helmis, C.G., Tombrou, M., Asimakopoulos, D.N., Soilemes, A., Güsten, H., Moussiopoulos, N. and Hatzaridou, A. (1997). Thessaloniki '91 Field Measurement Campaign-I. Wind Field and Atmospheric Boundary Layer Structure over Greater Thessaloniki Area, under Light Background Flow. *Atmos. Environ.* 31: 1101-1114.

Hertel, O., Christensen, J., Runge, E. H., Asman, W. A. H., Berkowicz, R., Hovmand M. F. and Hov, Ø. (1995). Development and Testing of a New Variable Scale Air Pollution Model-ACDEP. *Atmos. Environ.* 29: 1267-1290.

Hoff, R.M., Mickle, R.E. and Fung, C. (1995). Vertical Profiles of Ozone during the EMEFS I Experiment in Southern Ontario. *Atmos. Environ.* 29: 1735-1747.

Hung, I.F., Deshpande, C.G., Tsai C.J. and Huang, S.H. (2005). Spatial and Temporal Distribution of Volatile Organic Compounds Around an Industrial Park of Taiwan. *Aerosol Air Qual. Res.* 5: 141-153.

Kumar, U., Prakash, A. and Jain, V.K. (2008). A Photochemical Modeling Approach to Investigate O_3 Sensitivity to NO_x and VOCs in the Urban Atmosphere of Delhi. *Aerosol Air Qual. Res.* 8: 147-159.

Kuo, P.H., Ni, P.C., Keats, A., Tsuang, B.J., Lan, Y.Y., Lin, M.D., Chen, C.L., Tu, Y.Y., Chang, L.F. and Chang, K.H. (2009). Retrospective Assessment of Air Quality Management Practices in Taiwan. *Atmos. Environ.* (in press).

Lehning, M., Richner, H., Kok, G.L. and Neininger, B. (1998). Vertical Exchange and Regional Budgets of Air Pollutants over Densely Populated Areas. *Atmos. Environ.* 32: 1353-1363.

Lin, C.H. (2008). Impact of Downward Mixing Ozone Initially Existing in the Daily Atmosphere on Surface Ozone Accumulation in Southern Taiwan. *J. Air Waste Manage. Assoc.* 58: 562-579.

Lin, C.H., Lai, C.H., Wu, Y.L., Lai, H.C. and Lin, P. H. (2007). Vertical Ozone Distributions Observed Using Tethered Ozonesondes in a Coastal Industrial City, Kaohsiung, in Southern Taiwan. *Environ. Monit. Assess.* 127: 253-270.

Lin, C.H., Wu, Y.l., Lai, C.H., Lin, P.H., Lai, H.C. and Lin, P.L. (2004). Experimental Investigation of Ozone Accumulation Overnight during a Wintertime Ozone Episode in South Taiwan. *Atmos. Environ.* 38: 4267-4278.

Lin, C.H., Wu, Y.L., Lai, C.H., Watson, J.G. and Chow, J.C. (2008). Air Quality Measurements from the Southern Particulate Matter Supersite in Taiwan. *Aerosol Air Qual. Res.* 8: 233-264.

Ludwig, F.L., Jiang, J.Y. and Chen, J. (1995). Classification of Ozone and Weather Patterns Associated with High Ozone Concentrations in the San Francisco and Monterey Bay Areas. *Atmos. Environ.* 29: 2915-2928.

MacKenzie, A.R., Harrison, R.M., Colbeck, I., Clark, P.A. and Varey, R.H. (1995). The Ozone Increments in Urban Plumes. *Sci. Total Environ.* 159: 91-99.

McElroy, J.L. and Smith, T.B. (1986). Vertical Pollutant Distributions and Boundary Later Structure Observed by Airborne Lidar near the Complex Southern California Coastline. *Atmos. Environ.* 20: 1555-1566.

McKendry, I.G., Steyn, D.G., Lundgren, J., Hoff, R.M., Strapp, W., Anlauf, K., Froude, F., Martin, J.B., Banta, R.M. and Olivier, L.D. (1997). Elevated Ozone Layers and Vertical Down-Mixing over the Lower Fraser Valley, BC. *Atmos. Environ.* 31: 2135-2146.

Neter, J., Wassermann, W. and Kutner, M.H. (2004). *Applied Linear Regression Models* (4th ed.), McGraw-Hill/Irwin, New York.

Neu, U., Kunzle, T. and Wanner, H. (1994). On the Relation between Ozone Storage in the Residual Layer and Daily Variation in Near-Surface Ozone Concentration – A Case Study. *Boundary Layer Meteorol.* 69: 221-247.

Oke, T.R. (1987). Boundary Layer Climates. (2nd ed). Routledge, New York.

Padro, J., Hartog, G.D. and Neumann, H.H. (1991). An Investigation OH the ADOM Dry Deposition Module Using Summertime O_3 Measurements above a Deciduous Forest. *Atmo. Environ.* 25: 1689-1704.

Pisano, J.T., McKendry, I., Steyn, D.G. and Hastie, D.R. (1997). Vertical Nitrogen Dioxide and Ozone Concentrations Measured from a Tethered Balloon in the Lower Fraser Valley. *Atmos. Environ.* 31: 2071-2078.

Ryerson, T.B., Trainer, M., Holloway, J.S., Parrish, D.D., Huey, L.G., Sueper, D.T., Frost, G.J., Donnelly, S.G., Schauffler, S., Atlas, E.L., Kuster, W.C., Goldan, P.D., Hübler, G., Meagher, J.F. and Fehsenfeld, F.C. (2001). Observations of Ozone Formation in Power Plant Plumes and Implications for Ozone Control Strategies. *Science.* 292: 719-723.

Seibert, P., Beyrich, F., Gryning, S.E., Joffre, S., Rasmussen, A. and Tercier, P. (2000). Review and Intercomparison of Operational Methods for the Determination of the Mixing Height. *Atmo. Environ.* 34: 1001-1027.

Seinfeld, J.H. and Pandis, S.N. (1998). *Atmospheric Chemistry and Physics*. Wiley-Interscience Publication, New York, p. 1098-1099.

Silibello, C., Calori, G., Brusasca, G., Catenacci, G. and Finzi, G. (1998). Application of a Photochemical Grid Model to Milan Metropolitan Area. *Atmo. Environ.* 32: 2025-2038.

Stull, R.B. (1988). *An Introduction to Boundary Layer Meteorology*. Kluwer Atmosspheric Publ, Dordrecht, p. 670.

Tollefson, J. (2007). Countries with Highest CO_2-Emitting Power Sectors. *Nature*. 450: 327.

Tsai, J.L. and Tsuang, B.J. (2005). Aerodynamic Roughness over an Urban Area and over Two Farmlands in a Populated Area as Determined by Wind Profiles and Surface Energy Flux Measurements. *Agric. For. Meteorol.* 132: 154-170.

Tseng, K.H., Wang, J.L., Cheng, M.T. and Tsuang, B.J. (2009). Assessing the Relationship between Air Mass Age and Summer Ozone Episodes Based on Photochemical Indices. *Aerosol Air Qual. Res.* (in press).

Tsuang, B.J. (2003). A Gaussian Plume Trajectory Model to Quantify the Source/Receptor Relationship of Primary Pollutants and Secondary Aerosols: Part I. Theory. *Atmos. Environ.* 37: 3981-3991.

Tsuang, B.J. and Chao, C.P. (1999). Application of Circuit Model for Taipei City PM_{10} Simulation. *Atmos. Environ.* 33: 1789-1801.

Tsuang, B.J. and Chao, J.P. (1997). Development of a Circuit Model to Describe the Advection-Diffusion Equation for Air Pollution. *Atmos. Environ.* 31: 639-657.

Tsuang, B.J., Chen, C.L., Lin, C.H., Cheng, M.T., Tsai, Y.I., Chu, C.P., Pan, R.C. and Kuo, P.H. (2003). A Gaussian Plume Trajectory Model to Quantify the Source/Receptor Relationship of Primary Pollutants and Secondary Aerosols: Part II. Case Study. *Atmos. Environ.* 37: 3993-4006.

Vukovich, F.M. (1994). Boundary layer ozone variations in the eastern United States and their associations with meteorological variations: long-term variations. *J. Geophys. Res.* 99(D8): 16839-16850.

Wang, J.H., Chang, C.C. and Wang, J.L. (2005). Peak Tailoring Concept in GC Analysis of Volatile Organic Pollutants in the Atmosphere. *J. Chromatography A.* 1087: 150-157.

Wang, W.C. and Chen, K.S. (2008). Modeling and Analysis of Source Contribution of PM_{10} during Severe Pollution Events in Southern Taiwan. *Aerosol Air Qual. Res.* 8: 319-338.

Yang, D., Wang, Z. and Zhang, R. (2008). Estimating Air Quality Impacts of Elevated Point Source Emissions in Chongqing, China. *Aerosol Air Qual. Res.* 8: 279-294.

Yang, H.H., Chen, H.W., Chi, T.W. and Chuang, P.Y. (2008). Analysis of Atmospheric Ozone Concentration Trends as Measured by Eighth Highest Values. *Aerosol Air Qual. Res.* 8: 308-318.

Yang, K.L., Ting, C.C., Wang, J.L., Oliver, W.W. and Chan, C.C. (2005). Diurnal and Seasonal Cycles of Ozone Precursors Observed from Continuous Measurements at an Urban Site in Taiwan. *Atmos. Environ.* 39: 3221-3230.

Received for review, April 2, 2009
Accepted, May 27, 2009